

## OCEANOGRAPHY

# Most atolls will be uninhabitable by the mid-21st century because of sea-level rise exacerbating wave-driven flooding

Curt D. Storlazzi,<sup>1\*</sup> Stephen B. Gingerich,<sup>2</sup> Ap van Dongeren,<sup>3</sup> Olivia M. Cheriton,<sup>1</sup> Peter W. Swarzenski,<sup>4</sup> Ellen Quataert,<sup>3</sup> Clifford I. Voss,<sup>5</sup> Donald W. Field,<sup>6</sup> Hariharasubramanian Annamalai,<sup>7</sup> Greg A. Piniak,<sup>6</sup> Robert McCall<sup>3</sup>

Sea levels are rising, with the highest rates in the tropics, where thousands of low-lying coral atoll islands are located. Most studies on the resilience of these islands to sea-level rise have projected that they will experience minimal inundation impacts until at least the end of the 21st century. However, these have not taken into account the additional hazard of wave-driven overwash or its impact on freshwater availability. We project the impact of sea-level rise and wave-driven flooding on atoll infrastructure and freshwater availability under a variety of climate change scenarios. We show that, on the basis of current greenhouse gas emission rates, the nonlinear interactions between sea-level rise and wave dynamics over reefs will lead to the annual wave-driven overwash of most atoll islands by the mid-21st century. This annual flooding will result in the islands becoming uninhabitable because of frequent damage to infrastructure and the inability of their freshwater aquifers to recover between overwash events. This study provides critical information for understanding the timing and magnitude of climate change impacts on atoll islands that will result in significant, unavoidable geopolitical issues if it becomes necessary to abandon and relocate low-lying island states.

## INTRODUCTION

Recent observations (1, 2) and projections (3, 4) of sea level show that eustatic sea-level rise (SLR) by the end of the 21st century could exceed 2.0 m above 2000 levels. Although the precise rates and elevations of SLR by 2100 are uncertain, the existing models all suggest that eustatic sea level will be significantly higher by the end of the century and that it will have a profound impact on low-lying coastal areas. Projections indicate that these effects will be amplified in the tropics, where sea level will be higher than the global average (5). Furthermore, the tropics are dotted with thousands of low-lying atoll islands, and because many of these islands have maximum elevations less than 4 m and average elevations less than 2 m above present sea level, they are expected to experience disproportionately greater SLR impacts (6). Most atoll islands have limited adaptation space, land available for human habitation (7–9), and water and food sources (10, 11), and most have ecosystems that are vulnerable to seawater inundation (12). In addition, the majority of carbonate islands are positioned on coral reefs, where measured vertical reef flat accretion rates [2 to 6 mm/year; (13)] are up to an order of magnitude slower than the rates of projected SLR [8 to 20 mm/year; (3, 4)]. Projected SLR will, thus, outstrip new reef flat accretion, resulting in a net increase in water depth over atolls' reefs.

Wave impacts can be caused by events such as passing tropical storms and cyclones but can also occur as “blue sky events” due to large, remotely generated swell (9). SLR will exacerbate the impact of large waves on atolls' coral reefs by reducing wave breaking at the reef crest and increasing the water level over the reef flat, which will allow larger

waves to reach the shoreline [Fig. 1; (14, 15)]. These larger waves will increase wave-driven runoff and, thus, total water levels at the shoreline (15, 16). Wave-induced overwash and the resulting island flooding threaten terrestrial infrastructure (11) and can contaminate an island's underlying thin freshwater lens with saltwater (17, 18).

To date, most studies that describe future SLR threats to low-lying atoll islands (7, 8) generally have used passive models to simulate SLR inundation of the islands; these models do not incorporate the nonlinear interaction between SLR and waves (14, 15), let alone their interaction with island hydrogeology. Our study used field data to calibrate oceanographic and hydrogeologic models, which were then used with climate change and SLR projections to explore the effect of SLR and wave-driven flooding on atoll islands and their freshwater resources. The objective of this effort was to reduce risk and increase island resiliency by providing model simulations across a range of plausible future conditions, which have large uncertainty in future emissions (and thus climate change scenarios) that is largely irreducible. This effort focuses on Roi-Namur Island on Kwajalein Atoll in the Republic of the Marshall Islands (RMI), which is home to more than 1100 low-lying islands on 29 atolls. The approach and findings presented in this study can serve as a proxy for atolls around the world, most of which have a similar morphology and structure (including, on average, even lower land elevations) and are the home for numerous island nations and hundreds of thousands of people.

## RESULTS

Physics-based numerical oceanographic and hydrogeologic models are necessary to robustly assess how future SLR will affect wave-driven flooding and the resulting impacts to human populations, infrastructure, and freshwater resources on atoll islands. To make accurate projections, such modeling requires field data for validation and calibration. Roi-Namur, an island with a mean elevation of 2 m above mean sea level (Fig. 2A), was selected as the study site for this effort because it recently

Copyright © 2018  
The Authors, some  
rights reserved;  
exclusive licensee  
American Association  
for the Advancement  
of Science. No claim to  
original U.S. Government  
Works. Distributed  
under a Creative  
Commons Attribution  
NonCommercial  
License 4.0 (CC BY-NC).

Downloaded from <http://advances.sciencemag.org/> on April 30, 2018

<sup>1</sup>U.S. Geological Survey, Pacific Coastal and Marine Science Center, Santa Cruz, CA 95060, USA. <sup>2</sup>U.S. Geological Survey, Oregon Water Science Center, Portland, OR 97201, USA. <sup>3</sup>Deltares, Rotterdamseweg, Delft, Netherlands. <sup>4</sup>International Atomic Energy Agency (IAEA) Environment Laboratories, IAEA, Monaco, Principality of Monaco. <sup>5</sup>U.S. Geological Survey, National Research Program, Menlo Park, CA 94025, USA. <sup>6</sup>National Oceanic and Atmospheric Administration, National Ocean Service, National Centers for Coastal Ocean Science, Beaufort, NC 28516, USA. <sup>7</sup>International Pacific Research Center, University of Hawaii, Honolulu, HI 96822, USA. \*Corresponding author. Email: cstorlazzi@usgs.gov

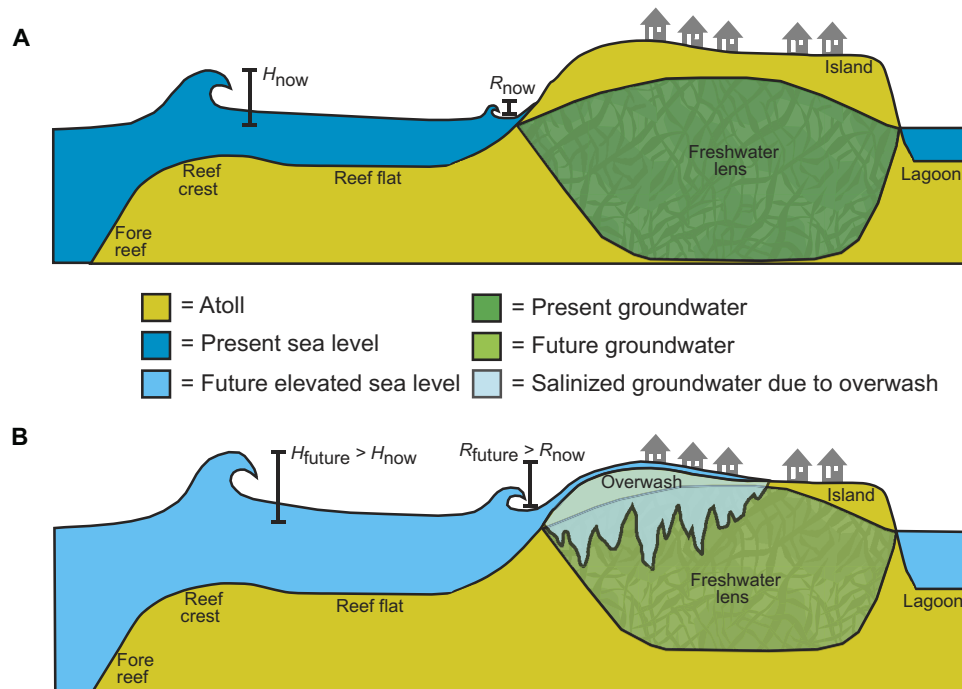


**Fig. 1. Conceptual diagram of the influence of SLR on wave heights, wave-driven runup, and flooding and the resulting impact on atoll island groundwater.** (A) Current sea level. (B) Future elevated sea level. SLR will allow for greater wave heights,  $H$ , and wave-driven runup,  $R$ , than at present, resulting in frequent overwash that will contaminate the atoll island's freshwater lens. High vertical exaggeration in schematic.

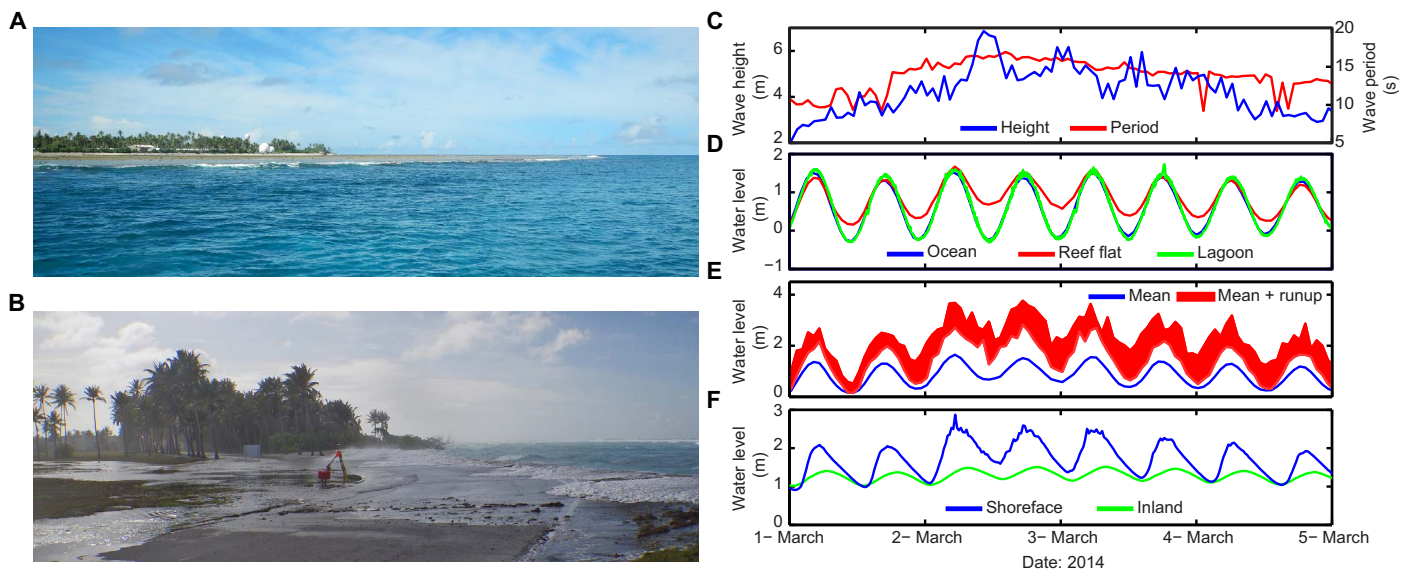


**Fig. 2. The morphology of Roi-Namur Island on Kwajalein Atoll and the impact of the March 2014 large wave event on the island's oceanography and hydrogeology.** (A) Photograph of the seaward side of Roi-Namur showing the wide coral reef flat and low relief of the island during typical low-energy conditions. (B) Photograph of the seaward side of Roi-Namur showing the wave-driven runup and seawater flooding inland (to the left) during the March 2014 large wave event. (C) Wave heights and wave periods offshore the island during the March 2014 large wave event. (D) Mean seawater levels across the atoll. (E) Instantaneous wave-driven water levels and modeled runup at the seaward shoreline. (F) Groundwater levels at a subset of the monitoring wells. At the peak of the 2 to 3 March large wave event, wave-driven flooding overwashed the seaward portion of the island, raising groundwater levels and salinizing portions of the island's freshwater lens.

experienced wave-driven marine flooding (9, 11) and an existing suite of groundwater monitoring wells provided a detailed understanding of the hydrogeology and groundwater resources (18). We conducted a field campaign on Roi-Namur from November 2013 to May 2015 to collect the requisite data to calibrate and validate the models.

Within the observational period, a large wave event (16), with wave heights exceeding 6 m, occurred on 2 to 3 March 2014. This wave event (Fig. 2, B and C) coincided with spring tides, which resulted in unusually elevated water levels over the atoll's reef flat (Fig. 2D) and anomalously large wave-driven runup at the shoreline (Fig. 2E). Together,

these conditions resulted in wave-driven shoreline water levels that exceeded the crest of the coastal berm; as a result, seawater overwashed parts of northern Roi-Namur and flooded inland into topographic lows (Fig. 2B). During the period of overwash, the groundwater levels on the shoreface of Roi-Namur increased almost 1 m above normal levels; observations farther inland also showed increases and elevated salinity, indicating that seawater infiltrated into the groundwater across the northern portion of the island (Fig. 2F).

To investigate future wave and water-level dynamics at the island scale, it is first necessary to understand how the regional meteorological and oceanographic conditions will evolve with a changing climate. These conditions were derived from global climate models (GCMs), providing information on annual changes in waves (19), rainfall, winds, and tropical cyclones (TCs). These metrics were then combined with SLR projections (4) to provide inputs for the island-scale models and regional context for the results. For the area around Kwajalein Atoll, deep-water wave heights and wind speeds are projected to decrease slightly. The frequency of TCs is projected to decrease, which is consistent with recent studies (20), but their intensity is predicted to increase. Although projected changes in the regional oceanographic patterns point to a slight reduction in the impact of waves to these islands, we demonstrate below that the effects of these changes will likely be insignificant in comparison to the impact of projected SLR in the region (4). Rainfall is expected to decrease slightly, as has been predicted throughout large swaths of the tropics (21), which would cause a reduction in freshwater availability and lengthen aquifer recharge (18).

Two different models were used to examine the effects of increasing sea levels, offshore wave forcing, coastal overwash, flooding, and freshwater lens contamination on Roi-Namur. The first was a high-resolution, two-dimensional (2D) hydrodynamic model (XBEACH) of the study area, which was used to simulate wave transformation across the reef flat and subsequent overwash and coastal flooding. The calibrated XBEACH model was used to assess the impacts of wave-driven flooding under three climate-change scenarios: Representative Concentration Pathways (RCP) 4.5 and RCP8.5, representing medium and high greenhouse concentration trajectory scenarios, respectively (22–23); and RCP8.5+icesheet collapse (4). The climate change scenarios were incorporated into the model by increasing mean sea level based on the SLR [tables S1 and S2; (4)] and wave projections [table S1; (19)]. The modeled time frame ranged from 2035 to 2105 at 10-year time steps.

The second model was a 3D groundwater model (SUTRA) that simulates the salinization and recovery processes of aquifers on low-elevation atoll islands. The SUTRA model was calibrated and validated using well data collected during a previous 2008 seawater-flooding event (9, 11). The simulated postflood evolution of the aquifer salinity after a seawater-flooding event indicates that the natural groundwater convection in the model is initiated as saline water infiltrates downward from the flooded area. When the simulated natural recharge from rainfall begins, fresh water accumulates at the water table and slowly pushes the intruded seawater deeper in the freshwater lens and toward the coast. For simulations of future years, the SUTRA model was forced by the multimodel ensemble output from the five best GCMs and the SLR scenarios (4).

The modeled future forcing conditions, coupled with the hydrodynamic and groundwater models, allow us to investigate the effects of wave-driven flooding on atoll island habitability and how these effects will change because of SLR and different climate change scenarios. With SLR alone (no wave-driven flooding considered), under the

RCP8.5+icesheet collapse scenario, the projected spatial extent of seawater inundation on Roi does not affect most of the island until the end of the 21st century (Fig. 3, A to C). In terms of effects on freshwater availability, with no wave-driven flooding, the groundwater simulations indicate that, even when sea level is 1.6 m above present, the groundwater salinity would be only mildly affected and would remain potable. With +1.6 m of SLR, parts of the interior of Roi become saturated to the ground surface because the freshwater lens floats increasingly higher relative to the ground surface. These areas were simulated as freshwater bodies that lost water to evaporation, resulting in higher salinities in the island's freshwater lens.

However, with higher sea levels, the island is projected to experience more severe annual wave-driven flooding events, during which seawater overtops the coastal berm resulting in increased inland flooding (Fig. 3, D to F). With both wave-driven flooding and SLR inundation, at a sea-level increase of just 0.4 m, much of the isthmus that connects Roi and Namur will be flooded annually, negatively affecting the infrastructure in this location. The groundwater simulations indicate that, with wave-driven flooding and progressively higher sea levels, the freshwater supply will be more adversely affected than from SLR alone: The postflood groundwater will become more saline, and the recovery times to potable water conditions will lengthen. A simulation of a 3-year period (dry, average, and wet years) at +0.4 m of SLR (Fig. 4) indicates that, after two consecutive years of annual wave-driven flooding, the freshwater lens does not recover from the seawater contamination because chloride levels in the lens remain above the potability threshold (250 mg/liter).

Thus, this “tipping point”—the time at which potable groundwater on Roi-Namur will be unavailable—is projected to be reached in the very near future, that is, within the life span of current residents and before 2030 for the RCP8.5+icesheet collapse climate scenario and within the 2030–2040 time frame for the RCP8.5 scenario and 2055–2065 for the RCP4.5 scenario. The 10-year ranges in these time frames take into account variability related to the El Niño–Southern Oscillation, which, in any given year, can cause regional sea level around Kwajalein to elevate or lower by 0.2 m for a few months (24).

Even if the groundwater supply were supplemented or replaced with another source (for example, desalinization or delivery of fresh water from elsewhere), annual wave-driven flooding would continue to disrupt infrastructure on Roi-Namur. Furthermore, most of the thousands of other populated atoll islands have far more limited options for managing their limited groundwater resources and are, therefore, even less resilient to SLR than the example provided here for Roi-Namur. When the mean sea level is 1.0 m higher than that at present because of SLR, at least 50% of the island is projected to be flooded annually. This secondary tipping point—when most of Roi's land would be flooded annually—is projected to be reached in the 2055–2065 time frame for the RCP8.5+icesheet collapse climate scenario, the 2060–2070 time frame for the RCP8.5 scenario, and sometime after 2105 for the RCP4.5 scenario (Fig. 5). More than 90% of the island's surface is projected to be flooded annually when the mean sea level is 1.8 m higher than that at present because of SLR, which will likely be reached in the 2075–2085 time frame for the RCP8.5+icesheet collapse scenario and in the 2090–2100 time frame for the RCP8.5 scenario.

## DISCUSSION

Past efforts that relied solely on passive SLR inundation modeling to predict when atolls will become uninhabitable suggest that many atoll islands may remain suitable for human habitation until 2100 or 2150

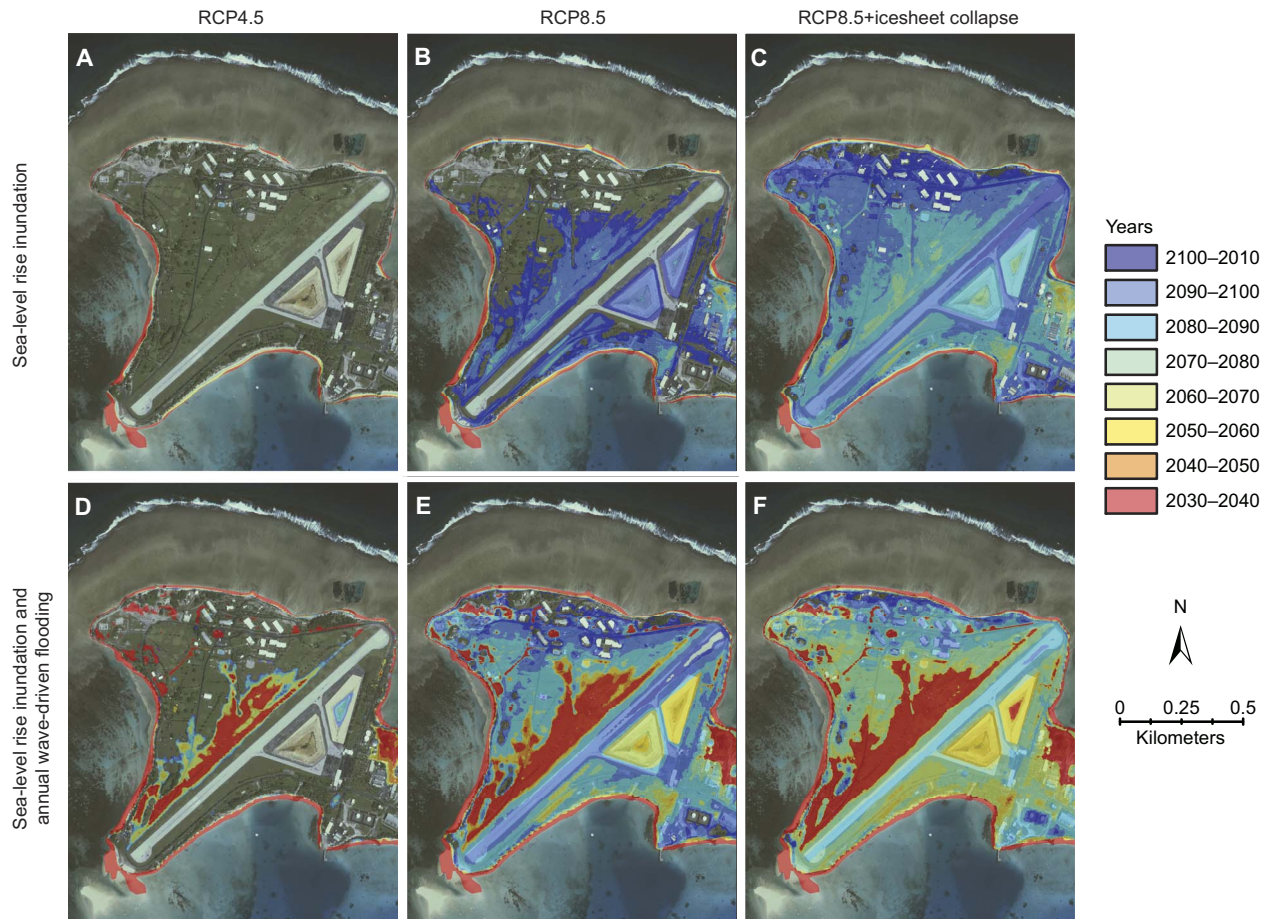


**Fig. 3. The projected spatial extent of inundation due to SLR and annual flooding due to the combined effects of waves and SLR on Roi through time for different SLR and climatic scenarios.** (A) SLR inundation for RCP4.5. (B) SLR inundation for RCP8.5. (C) SLR inundation for RCP8.5+icesheet collapse. (D) Annual wave-driven flooding for RCP4.5. (E) Annual wave-driven flooding for RCP8.5. (F) Annual wave-driven flooding for RCP8.5+icesheet collapse. The overwash extents during annual large wave events increase into the future because of SLR and with increasing RCP scenario; the island is completely overwashed annually by wave-driven flooding later in the 21st century for RCP8.5 scenarios.

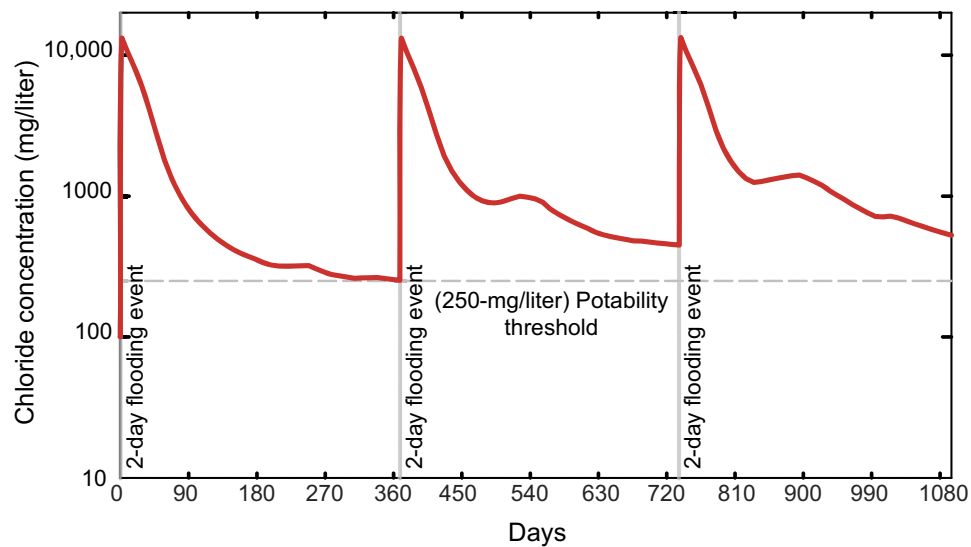


**Fig. 4. The forecasted impact of annual wave-driven flooding events on groundwater potability over 3 years for +0.4 m of SLR.** Plot shows the modeled evolution of chloride concentrations relative to the 250-mg/liter potability threshold. Within 2 years of annual flooding with +0.4 m of SLR, the island’s groundwater is no longer potable because of seawater contamination.

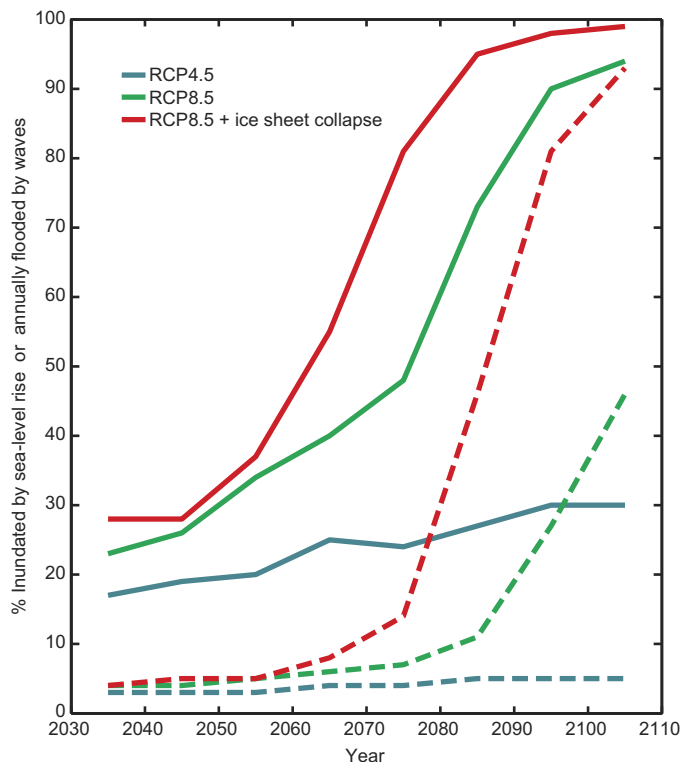


**Fig. 5. The projected percentage of Roi inundated because of SLR and flooded annually because of the combined effects of waves and SLR through time for different SLR and climatic scenarios.** Dashed lines denote percentage of the island inundated by SLR, and the solid lines denote that annually flooded by waves. Large portions of the island are only affected by inundation due to SLR later in the 21st century, if at all, whereas significant portions are annually flooded by waves by the latter half of the 21st century for the RCP8.5 scenarios. Wave-driven flooding of more than 25% of the island, however, is enough to contaminate the groundwater and make it nonpotable, which is forecasted to be attained by the mid-21st century for the RCP8.5 scenarios and the latter half of the 21st century for the RCP4.5 scenario.

(8). The results presented here, however, demonstrate that when the nonlinear interaction between SLR and wave-driven overwash and the subsequent island flooding are taken into account, the timeline for sustainable human habitation on these low-lying atoll islands shortens considerably. Not only will such flooding affect terrestrial infrastructure and habitats, but also, more importantly, it will make the limited freshwater resources nonpotable and, therefore, directly threaten the sustainability of human populations. On the basis of the limited topographic (7–10) and hydrogeologic (10, 17, 25) data available for atoll islands, Roi-Namur is characteristic of (if not of higher elevation than) most of the thousands of atoll islands in the world's oceans. Assuming that this is the case, then the tipping point, at which point potable groundwater on most of the atoll islands will be unavailable, is projected to be reached by no later than the 2030s for the RCP8.5+ice-sheet collapse climate scenario, by the 2040s for the RCP8.5 scenario, and 2060s for the RCP4.5 scenario. Island inhabitants will therefore be unable to rely on groundwater, in many cases the sole source of fresh water, as a source of potable water in the next few decades, and thus, the islands will be uninhabitable by the middle of the 21st century—not by the end of the 21st century or the middle of the 22nd century as previously suggested (8).

For those rare atoll islands where groundwater is not a limiting resource due to rainfall capture, desalination facilities, transport from elsewhere, etc., the tipping point at which most of those atoll islands would be flooded annually is projected to be reached in the 2060s for the RCP8.5+icesheet collapse climate scenario, the 2070s time frame for the RCP8.5 scenario, and sometime after the 2110s for the RCP4.5 scenario. These findings have relevance not only to populated atoll islands in the Marshall Islands but also to those in the Caroline Islands, Cook Islands, Gilbert Islands, Line Islands, Society Islands, Spratly Islands, Maldives, Seychelles, and Northwestern Hawaiian Islands. In addition, because the mid-Holocene sea-level highstand was highest in the Marshall Islands (8), providing the greatest vertical accommodation space for coral reefs to grow up into, the Marshall Islands are likely some of the highest atolls in the Pacific. Therefore, the timing of the tipping points presented here may be conservative (later in the future) compared to most of the other atoll islands that formed under lower mid-Holocene sea levels and, thus, have lower elevations. Islands fronted by wider, shallower reef flats with high coral coverage will have tipping points further in the future, whereas islands with narrower, deeper reef flats with lower coral cover (15) will reach these tipping points sooner than described here for Roi-Namur. Last, if coral bleaching events (26) and ocean acidification (27) also increase in frequency and/or magnitude because of global climate change, then live coral coverage will decline, resulting in increased depths and reduced hydrodynamic roughness of the reefs. This will further enhance wave energy propagation to the shoreline and subsequent wave-driven flooding (14–16), causing tipping points to be reached sooner than projected here.

Although the focus of the effort presented here is on low-lying coral atoll islands, our findings are relevant to other tropical, reef-lined islands. Because most high tropical islands such as those found in the Pacific, Atlantic, and Indian Oceans receive enough rainfall on their mountains to generate freshwater resources at elevations unreachable by wave-driven runoff, wave-driven coastal flooding will likely not threaten their freshwater resources. However, because most of these islands' housing and critical infrastructure (ports, roads, airports, hospitals, power plants, water treatment plants, etc.) are located within a few meters of current sea level, they are also vulnerable to increased wave-driven overwash due to SLR.

These projections of low-lying atoll island sustainability through the 21st century contrast with the recent hypotheses (28, 29) that islands will endure through the SLR projected through the end of the 21st century (3, 4). Those hypotheses were based on observations of how uninhabited islands' planform areas migrated but maintained themselves over a period of limited (<0.3 m) SLR during the 20th century. However, our results, as well as those from other studies (15, 16), demonstrate that a more critical metric than island planform area is the elevation of the island above the current sea level, because that elevation controls the frequency and magnitude of wave-driven overwash and island flooding. Although studies (7, 28) have shown that storms and wave-driven overwash can contribute to island formation through the deposition of reef-derived sediment during energetic events, the maximum vertical thickness of a storm or tsunami deposit is generally less than 10% and no more than 50% of the depth of the flooding seawater during the overwash event (30). Thus, wave-driven island overwash, subsequent flooding, and groundwater salinization (and saltwater intrusion) will continue to increase with SLR, despite any wave-driven sediment deposition. Although these islands may experience a variety of sediment deposition and/or migration patterns, including the maintenance of their lateral extents, because of the loss of freshwater resources

and the increased frequency of impacts to infrastructure, most of these islands will likely become uninhabitable in the near future, well before the end of the 21st century, as has been previously suggested (8).

Together, these results provide an improved and updated timeline of the threats that these low-lying atoll islands face to their infrastructure and natural resources in the face of future climate change. By incorporating wave-driven overwash into future predictions, we demonstrate the immediacy of the threats and underscore the urgency for planning and action. The next step is to use these results and those from theoretical simulations covering the range of reef island morphologies and climate forcing conditions to identify individual islands that are most vulnerable to SLR and then gauge the associated impacts to those islands over the next 20 to 50 years so that managers can prioritize funding for further place-based studies and/or restoration and adaptation efforts (11, 31). Although there are a number of engineering solutions to increase the resilience of infrastructure and food and water resources that could be used to help the islands adapt to climate change and extend their habitability, these solutions in remote areas generally have such high costs that most islands cannot afford them. This information will also be critical to political leaders, not only of island nations but also globally, for understanding how climate change will determine when these islands will no longer be able to support human habitation, resulting in an extensive displacement of human populations. If these impacts are not addressed or adequately planned for, as it becomes necessary to abandon or relocate island nations, then significant geopolitical issues could arise.

## MATERIALS AND METHODS

The primary goal of this investigation was to determine the influence of climate change and SLR on wave-driven flooding and the resulting impacts to infrastructure and freshwater resources on atoll islands. First, we mapped the morphology and benthic habitats of the atoll to determine the influence of spatially varying bathymetric structure and hydrodynamic roughness on wave propagation over the coral reefs that made up the atoll. Second, we analyzed historic meteorologic and oceanographic data to provide historical context for the limited in situ data and comparison to previous seawater overwash and flooding events. These data were then used to calibrate and validate physics-based, dynamically downscaled numerical models to project future atmospheric and oceanic forcing for a range of climate change scenarios. Third, we made in situ observations to better understand how changes in meteorologic and oceanographic forcing controlled wave-driven water levels, seawater flooding of the island, and the resulting hydrogeologic response. We then used those data to calibrate and validate physics-based, numerical hydrodynamic, and hydrogeologic models of the island. The hydrodynamic model was used to forecast future wave-driven island overwash and seawater flooding for a range of climate change and SLR scenarios. The output of those hydrodynamic simulations was then used as input to the hydrogeologic model to evaluate the impact of projected wave-driven flooding on the atoll island's freshwater resource and at what rate the resource can recover. Last, we projected the tipping points—when the reoccurrence interval of island overwash and seawater intrusion events is shorter than the recovery times for the impact.

### Mapping

The hydrodynamic and hydrogeologic models needed to be run on a high-resolution, seamless topographic and bathymetric (TB) digital el-

evation model (DEM) of the study area. To create the TB-DEM, topographic data from Global Positioning System (GPS) and terrestrial lidar scanning (TLS) collected on the island were combined with bathymetry derived from satellite imagery. The topographic surveys of Roi were conducted using static Topcon GRS1 dual-frequency GPS and GPS rovers. TLS surveys were conducted using a Riegl VZ-1000 tripod-based lidar scanner placed at 31 locations on the island. Data point cloud cleaning and filtering were performed on the registered point clouds to produce a subset of ground measurements suitable for constructing a bare-earth DEM. Because of the lack of high-resolution bathymetric data for the study area, WorldView-2 and WorldView-3 multispectral satellite imagery were used to derive bathymetry (32). Depths on the ocean side were a combination of depths generated from the model down to 22.5 m; past that, depths were taken from an interpolated surface from fathometer measurements. A  $3 \times 3$  low-pass convolution filter was used on the final product to eliminate single-pixel anomalies. To create the seamless TB-DEM of Roi-Namur, TLS, GPS, and satellite-derived bathymetry were combined into a 0.5-m grid. For the island and intertidal reef flat areas, TLS and GPS data were combined into a triangulated irregular network model. Because of the higher data density, TLS data were used preferentially over GPS and satellite-derived bathymetry wherever it was available. To produce the final seamless 0.5-m resolution TB-DEM, the onshore and offshore grids were combined.

Hydrodynamic modeling uses a variety of equations with different coefficients to describe interactions between waves, current, and the seabed. Benthic habitats were mapped using spectral classification with the Iterative Self-Organizing Data Analysis Technique (ISODATA) unsupervised clustering algorithm, in combination with on-screen, heads-up digitizing (33). The minimum mapping unit (MMU) in the areas where ISODATA was used to depths of 10 m was at the pixel level ( $4 \text{ m}^2$ ); the MMU in the deeper areas where on-screen digitizing was used was  $30 \text{ m}^2$ . The benthic habitat map was produced using a non-hierarchical classification system similar to the scheme used on adjacent Majuro Atoll (33). The resulting habitat map was converted to a spatially varying friction coefficient map, using published values for coral reef habitats from the literature (15, 34).

Land-cover data were needed to determine how much of any given land cover class would be inundated for a given future wave and sea-level scenario. Half-meter true-color and three-band color infrared satellite imagery were used as base layers to develop the terrestrial land-cover map. The ArcGIS Interactive Supervised Classification tool was used to delineate 15 distinct land-cover classes, and a majority filter was applied using eight closest cells. The result of the majority filter was a raster that was converted to polygons that were grouped by land-cover classification.

### Future oceanographic modeling

The potential future changes in ocean surface storm waves were quantitatively simulated using models driven by historical hindcast data and projected conditions based on GCM output (19). Three-hour GCM wind speed and wind direction output were assimilated for the area encompassing Kwajalein Atoll from the Coupled Model Intercomparison Project Phase 5 [CMIP5; (35)]. To reduce uncertainty in model variability, wind speed and wind direction for the RCP4.5 and RCP8.5 climate scenarios (table S1) from four different GCMs (table S3) were used as boundary conditions to the physics-based WAVEWATCH III (36) numerical wave model. Modeled time periods were limited to the years 2026–2045 and 2085–2100, as prescribed by the CMIP5 modeling

framework, and interpolated to the 2035–2105 time frame at 10-year time steps. The resulting modeled deep-water wave heights, wave periods, wave directions, wind speeds, and wind directions were analyzed using published methods (19).

### Oceanographic data acquisition

To calibrate and validate the physics-based, numerical nearshore hydrodynamic model, an 18-month field experiment was conducted on Roi-Namur Island in Kwajalein Atoll, and concurrent far-field, deep-water wave and wind-forcing data were acquired. Together, these observations elucidated the influence of water depth (as related to tidal and atmospheric forcing) on wave propagation and transformation across the atoll rim and over the reef flats for a range of oceanographic and meteorologic conditions. The 18-month field experiment consisted of three consecutive 6-month deployments in which two cross-shore arrays (16) were installed on the north, oceanside coastline of Roi (western portion of Roi-Namur). Each cross-shore array consisted of three bottom-mounted RBR wave/tide gauges over the reef flat and one on the upper fore reef. Between the two adjacent transects, an upward-looking 600-kHz Nortek Acoustic Wave and Current meter was placed on the fore reef. In addition, to capture wave and tidal conditions in the lagoon, an RBR wave/tide gauge and an RBR tide gauge were placed on a dock pier.

### Wave-driven flood modeling

XBEACH is a high-fidelity, physics-based, nonhydrostatic, 2D area model for the nearshore and coast (15, 34). A high-resolution (2- to 50-m grid cells with the finest scale on the island) implementation of XBEACH was used to simulate wave transformation and coastal flooding on Roi-Namur. The XBEACH model was calibrated and validated by comparing modeled and measured wave and water-level data from the December 2013 and March 2014 large wave events. The calibrated and validated XBEACH model was then forced with SLR values (4) that ranged from +0.2 to +2.9 m (tables S1 and S2). The incident offshore wave parameters used in the model (19) had offshore wave heights ranging from 2.2 to 5.1 m and periods from 11 to 15 s. The modeled years ranged from 2035 to 2105 at 10-year intervals, and the SLR and wave parameters used for each year were based on interpolation of the SLR (4) and future wave (19) projections. To include the effect of higher bottom roughness on incident wave decay, a spatially varying friction coefficient was incorporated on the basis of the benthic habitat mapping. The 2D model was calibrated for the current friction coefficient by comparing modeled and measured in situ wave and water-level data and the spatially varying habitat data.

### Future climate modeling

The availability of multimember ensembles of present-day and warming scenario simulations from 41 GCMs (table S3) in CMIP5 (35) provides a unique opportunity to examine the ability of global models to accurately represent climate, both in terms of future predictions and the observed long-term trends in the tropical Pacific and Indian Ocean regions over recent decades. Historical simulations (1971–2005) were used to assess the models' ability to realistically simulate the annual mean precipitation, winds, sea surface temperatures (SSTs), and their annual cycles. On the basis of a suite of metrics, five models that demonstrated high skills ("best") in representing the present-day climatology and variability (table S3) were selected from the larger pool of 41 GCMs for detailed analyses. Then, for the five best GCMs, their skill in capturing interannual variations in seasonal rainfall during rainy seasons was examined. Final-

ly, mean annual changes in rainfall, SST, and winds from the five best GCMs were used for future projections. Although CMIP5 global models do not adequately simulate the intensity of fully developed tropical cyclones (TCs), the genesis and the early life of TCs, in these models over the west Pacific were evaluated, and the statistical properties of these storms around Kwajalein were quantified. The TRACK program (37), a mathematically and physically developed objective procedure, was applied on the model output to diagnose tropical storms over the west Pacific region. TRACK objectively identifies TCs through analysis of the time series of meteorological fields.

### Groundwater data acquisition

An assessment of the Roi-Namur shallow groundwater lens was carried out from November 2013 to April 2015. This assessment included surveys of groundwater levels, temperature, and specific conductivity (salinity) in a suite of wells and temporary piezometers strategically placed around the island to provide time-series groundwater levels and specific conductivity measurements. In addition, depth-specific groundwater samples were collected.

### Groundwater modeling

We developed framework for simulating the salinization and recovery processes that affect freshwater supply on low-elevation atoll islands. A 3D finite-element model of variable-density groundwater flow and salt transport in the island aquifer was created using the U.S. Geological Survey (USGS) SUTRA groundwater model (38). The model domain includes Roi and some distance offshore to a depth of about 105 m below sea level. The TB-DEM was used as the SUTRA model's surface. For this model, the SUTRA code was modified to account for water table storage by including the aquifer-specific yield in the governing equations. The SUTRA model was calibrated and validated using observations from a December 2008 wave-driven overwash and flooding event on Roi-Namur.

### Flood modeling and groundwater response

The future impacts of seawater overwash and subsequent flooding on the freshwater lens were investigated using the SUTRA model (18). These simulations take into account various stages of higher sea level, estimated saltwater ponding over the surface of Roi, and natural recharge of wells via rainfall. The annual wave events derived from the future oceanographic flood modeling were used to drive overwash. Then, following these overwash events, the temporal evolution of the freshwater-lens seawater contamination (chloride concentrations relative to potability levels) was simulated with the same groundwater pumping rate and timing as occurred in the years following the 2008 flooding event. Future recharge (2080–2099) was estimated using rainfall and evapotranspiration based on future climate modeling of the RCP8.5 scenario. Modeled climate data were processed for historic (1990–2009) and future (2080–2099, RCP8.5) conditions to compute mean monthly change factors for rainfall amount, number of rain days, and reference evapotranspiration to compute recharge for future conditions.

Future sea levels and worst-case annual seawater flooding scenarios were estimated as described in the "Wave-driven flood modeling" section. SLR scenarios of +0.4, +0.8, +1.2, and +1.6 m (RCP8.5 estimates of SLR at Roi-Namur in 2035, 2055, 2075, and 2090, respectively) and the associated annual wave-driven flooding were simulated. For each scenario, the coastline of the island was reduced accordingly on the basis of island topography, and then the estimated maximum seawater

flooding distribution was applied to the model for a 2-day period each year. The response of the freshwater lens was evaluated on the basis of how the salinity (chloride concentration) of water at the skimming well changed during the recovery time period. Under some climatic scenarios, it was necessary to carry out these simulations for several years after a single overwash event so that the full duration of the lens recovery could be resolved. Finally, simulations of three consecutive years of annual overwash and flooding events during dry, average, and wet recharge conditions with representative withdrawal patterns for each year were completed.

### Statistical analyses

The statistical methods used in this study were published as follows: mapping and bathymetry generation (32), oceanographic measurements (16), hydrogeologic measurements (39), future oceanographic modeling (19), future wave-driven flood modeling (15), future meteorologic modeling (37), and future groundwater modeling (18, 38).

### SUPPLEMENTARY MATERIALS

Supplementary material for this article is available at <http://advances.sciencemag.org/cgi/content/full/4/4/eaap9741/DC1>

table S1. Overview of SLR (4) and wave (19) projections per climate change scenario for each year used in the XBEACH wave-driven flood modeling.

table S2. SLR scenarios and their contributions by year and climate change scenario (4).

table S3. List of GCMs analyzed and used as input data for the regional climatic (37)

and oceanographic (19) models and local oceanographic (15) and hydrogeologic (18, 38) models.

### REFERENCES AND NOTES

- S. Jevrejeva, A. Grinsted, J. C. Moore, Anthropogenic forcing dominates sea-level rise since 1850. *Geophys. Res. Lett.* **36**, L20706 (2009).
- M. Vermeer, S. Rahmstorf, Global sea level linked to global temperature. *Proc. Natl. Acad. Sci. U.S.A.* **106**, 21527–21532 (2009).
- R. E. Kopp, R. M. Horton, C. M. Little, J. X. Mitrovica, M. Oppenheimer, D. J. Rasmussen, B. H. Strauss, C. Tebaldi, Probabilistic 21st and 22nd century sea-level projections at a global network of tide-gauge sites. *Earths Future* **2**, 383–406 (2014).
- J. A. Hall, S. Gill, J. Obeysekera, W. Sweet, K. Knutti, J. Marburger, *Regional Sea Level Scenarios for Coastal Risk Management: Managing the Uncertainty of Future Sea Level Change and Extreme Water Levels for Department of Defense Coastal Sites Worldwide* (U.S. Department of Defense, Strategic Environmental Research and Development Program, 2016).
- A. B. A. Slangen, M. Carson, C. A. Katsman, R. S. W. van de Wal, A. Köhl, L. L. A. Vermeersen, D. Stammer, Projecting twenty-first century regional sea-level changes. *Clim. Change* **124**, 317–332 (2014).
- S. Vitousek, P. L. Barnard, C. H. Fletcher, N. Frazer, L. Erikson, C. D. Storlazzi, Doubling of coastal flooding frequency within decades due to sea-level rise. *Sci. Rep.* **7**, 1399 (2017).
- C. D. Woodroffe, Reef-island topography and the vulnerability of atolls to sea-level rise. *Glob. Planet. Change* **62**, 77–96 (2008).
- W. R. Dickinson, Pacific atoll living: How long already and until when? *GSA Today* **19**, 4–10 (2009).
- R. K. Hoeke, K. L. McInnes, J. C. Kruger, R. J. McNaught, J. R. Hunter, S. G. Smithers, Widespread inundation of Pacific islands triggered by distant-source wind-waves. *Glob. Planet. Change* **108**, 128–138 (2013).
- R. T. Bailey, J. W. Jenson, A. E. Olsen, Estimating the ground water resources of atoll islands. *Water* **2**, 1–27 (2010).
- C. H. Fletcher, B. M. Richmond, *Climate Change in the Federated States of Micronesia: Food and Water Security, Climate Risk Management, and Adaptive Strategies* (University of Hawaii Sea Grant Report TT-10-02, 2010).
- M. H. Reynolds, K. N. Courtot, P. Berkowitz, C. D. Storlazzi, J. Moore, E. Flint, Will the effects of sea-level rise ecological traps for Pacific island seabirds? *PLOS ONE* **10**, e0136773 (2015).
- L. F. Montaggioni, History of Indo-Pacific coral reef systems since the last glaciation: Development patterns and controlling factors. *Earth Sci. Rev.* **71**, 1–75 (2005).
- C. D. Storlazzi, E. Elias, M. E. Field, M. K. Presto, Numerical modeling of the impact of sea-level rise on fringing coral reef hydrodynamics and sediment transport. *Coral Reefs* **30**, 83–96 (2011).
- E. Quataert, C. Storlazzi, A. van Rooijen, O. Cheriton, A. van Dongeren, The influence of coral reefs and climate change on wave-driven flooding of tropical coastlines. *Geophys. Res. Lett.* **42**, 6407–6415 (2015).
- O. M. Cheriton, C. D. Storlazzi, K. J. Rosenberger, Observations of wave transformation over a fringing coral reef and the importance of low-frequency waves and offshore water levels to runup, overwash, and coastal flooding. *J. Geophys. Res. Oceans* **121**, 3121–3140 (2016).
- J. P. Terry, A. C. Falkland, Response of atoll freshwater lenses to storm-surge overwash in the Northern Cook Islands. *Hydrogeol. J.* **18**, 749–759 (2010).
- S. B. Gingerich, C. I. Voss, A. G. Johnson, Seawater-flooding events and impact on freshwater lenses of low-lying islands: Controlling factors, basic management and mitigation. *J. Hydrol.* **551**, 676–688 (2017).
- J. B. Shope, C. D. Storlazzi, L. H. Erikson, C. A. Hegermiller, Changes to extreme wave climates of islands within the Western Tropical Pacific throughout the 21st century under RCP 4.5 and RCP 8.5, with implications for island vulnerability and sustainability. *Glob. Planet. Change* **141**, 25–38 (2016).
- T. R. Knutson, J. L. McBride, J. Chan, K. Emanuel, G. Holland, C. Landsea, I. Held, J. P. Kossin, A. K. Srivastava, M. Sugi, Tropical cyclones and climate change. *Nat. Geosci.* **3**, 157–163 (2010).
- K. B. Karnauskas, J. P. Donnelly, K. J. Anchukaitis, Future freshwater stress for island populations. *Nat. Clim. Chang.* **6**, 720–725 (2016).
- K. Riahi, V. Krey, S. Rao, V. Chirkov, G. Fischer, P. Kolp, G. Kindermann, N. Nakicenovic, P. Rafai, RCP-8.5: Exploring the consequence of high emission trajectories. *Clim. Change* **109**, 33–57 (2010).
- A. M. Thomson, K. V. Calvin, S. J. Smith, G. P. Kyle, A. Volke, P. Patel, S. Delgado-Arias, B. Bond-Lamberty, M. A. Wise, L. E. Clarke, J. A. Edmonds, RCP4.5: A pathway for stabilization of radiative forcing by 2100. *Clim. Change* **109**, 77–94 (2010).
- M. R. Chowdhury, P.-S. Chu, T. Schroeder, ENSO and seasonal sea-level variability—a diagnostic discussion for the U.S.-Affiliated Pacific Islands. *Theor. Appl. Climatol.* **88**, 213–224 (2007).
- M. R. Underwood, F. L. Peterson, C. I. Voss, Groundwater lens dynamics of Atoll Islands. *Water Resour. Res.* **28**, 2889–2902 (1992).
- L. Teneva, M. Karnauskas, C. A. Logan, L. Bianucci, J. C. Currie, J. A. Kleypas, Predicting coral bleaching hotspots: The role of regional variability in thermal stress and potential adaptation. *Coral Reefs* **31**, 1–12 (2012).
- J. M. Pandolfi, S. R. Connolly, D. J. Marshall, A. L. Cohen, Projecting coral reef futures under global warming and ocean acidification. *Science* **333**, 418–422 (2011).
- M. R. Ford, P. S. Kench, Multi-decadal shoreline change in response to sea level rise in the Marshall Islands. *Anthropocene* **11**, 14–24 (2015).
- P. S. Kench, D. Thompson, M. R. Ford, H. Ogawa, R. F. McLean, Coral islands defy sea-level rise over the past century: Records for a central Pacific atoll. *Geology* **43**, 515–518 (2015).
- R. A. Morton, G. Gelfenbaum, B. E. Jaffe, Physical criteria for distinguishing sandy tsunami and storm deposits using modern examples. *Sediment. Geol.* **200**, 184–207 (2007).
- N. Mimura, Vulnerability of island countries in the South Pacific to sea level rise and climate change. *Clim. Res.* **12**, 137–143 (1999).
- R. P. Stumpf, K. Holderied, M. Sinclair, Determination of water depth with high-resolution satellite imagery over variable bottom types. *Limnol. Oceanogr.* **48**, 547–556 (2003).
- M. S. Kendall, T. A. Battista, C. Menza, *Majuro Atoll, Republic of the Marshall Islands Coral Reef Ecosystems Mapping Report* (NOAA National Centers for Coastal Ocean Science, Center for Coastal Monitoring, Biogeography Branch, NOAA Technical Memorandum, NOS NCCOS 144, 2012).
- A. Van Dongeren, R. Lowe, A. Pomeroy, D. M. Trang, D. Roelvink, G. Symonds, R. Ranasinghe, Numerical modeling of low-frequency wave dynamics over a fringing coral reef. *Coast. Eng.* **73**, 178–190 (2013).
- World Climate Research Programme, *CMIP5–Coupled Model Intercomparison Project, Phase 5 overview* (2012); <http://cmip-pcmdi.llnl.gov/cmip5/>.
- H. L. Tolman, *User manual and system documentation of WAVEWATCH III version 3.14* (NOAA/NWS/NCEP/MMAB Technical Note 276, 2009).
- K. I. Hodges, Confidence intervals and significance tests for spherical data derived from feature tracking. *Mon. Weather Rev.* **136**, 1758–1777 (2008).
- C. I. Voss, A. M. Provost, *SUTRA: A model for saturated-unsaturated variable-density ground-water flow with solute or energy transport, Version of September 22, 2010* (U.S. Geological Survey Water-Resources Investigations Report 02-4231, 2002).
- F. K. J. Oberle, P. W. Swarzenski, C. D. Storlazzi, Atoll groundwater movement and its response to climatic and sea-level fluctuations. *Water* **9**, 650 (2017).

**Acknowledgments:** We would like to thank Strategic Environmental Research and Development Program (SERDP) staff and the U.S. Army Garrison–Kwajalein Atoll for their overarching support of this project. Any use of trade, firm, or product names is for descriptive purposes only and does not imply endorsement by the U.S. government. **Funding:** This work was funded by the U.S. Department of Defense's SERDP as project RC-2334, the USGS Coastal and Marine Geology Program, and Deltares Strategic Research in the "Hydro- and morphodynamics during extreme events" program (11200604). **Author contributions:** C.D.S., S.B.G., A.v.D., P.W.S., D.W.F., H.A., and G.A.P. designed the research; C.D.S., S.B.G., A.v.D., O.M.C., P.W.S., E.Q., C.I.V., R.M., D.W.F., H.A., and G.A.P. carried out the research; C.D.S., S.B.G., A.v.D., O.M.C., P.W.S., E.Q., C.I.V., R.M., D.W.F., H.A., and G.A.P. conducted the analyses; and C.D.S., S.B.G., A.v.D., O.M.C., P.W.S., D.W.F., H.A., and G.A.P. wrote the paper. **Competing interests:** The authors declare that they have no competing interests. **Data and materials availability:** All data needed to evaluate the conclusions in the paper are present in the

paper and/or the Supplementary Materials. Additional data related to this paper is available at the Science Base webpage (<https://doi.org/10.5066/F7VD6XDB>) or may be requested from the authors.

Submitted 15 September 2017

Accepted 9 March 2018

Published 25 April 2018

10.1126/sciadv.aap9741

**Citation:** C. D. Storlazzi, S. B. Gingerich, A. van Dongeren, O. M. Cheriton, P. W. Swarzenski, E. Quataert, C. I. Voss, D. W. Field, H. Annamalai, G. A. Piniak, R. McCall, Most atolls will be uninhabitable by the mid-21st century because of sea-level rise exacerbating wave-driven flooding. *Sci. Adv.* **4**, eaap9741 (2018).

## Most atolls will be uninhabitable by the mid-21st century because of sea-level rise exacerbating wave-driven flooding

Curt D. Storlazzi, Stephen B. Gingerich, Ap van Dongeren, Olivia M. Cheriton, Peter W. Swarzenski, Ellen Quataert, Clifford I. Voss, Donald W. Field, Hariharasubramanian Annamalai, Greg A. Piniak and Robert McCall

*Sci Adv* 4 (4), eaap9741.  
DOI: 10.1126/sciadv.aap9741

### ARTICLE TOOLS

<http://advances.sciencemag.org/content/4/4/eaap9741>

### SUPPLEMENTARY MATERIALS

<http://advances.sciencemag.org/content/suppl/2018/04/23/4.4.eaap9741.DC1>

### REFERENCES

This article cites 33 articles, 3 of which you can access for free  
<http://advances.sciencemag.org/content/4/4/eaap9741#BIBL>

### PERMISSIONS

<http://www.sciencemag.org/help/reprints-and-permissions>

Use of this article is subject to the [Terms of Service](#)

---

*Science Advances* (ISSN 2375-2548) is published by the American Association for the Advancement of Science, 1200 New York Avenue NW, Washington, DC 20005. 2017 © The Authors, some rights reserved; exclusive licensee American Association for the Advancement of Science. No claim to original U.S. Government Works. The title *Science Advances* is a registered trademark of AAAS.